All-atomic source of squeezed vacuum with full pulse-shape control

2012 J. Phys. B: At. Mol. Opt. Phys. 45 124015

(http://iopscience.iop.org/0953-4075/45/12/124015)

J. Phys. B: At. Mol. Opt. Phys. **45** (2012) 124015 (6pp) doi:10.1088/0953-4075/45/12/124015

All-atomic source of squeezed vacuum with full pulse-shape control

Travis Horrom, Irina Novikova and Eugeniy E Mikhailov[1]

College of William and Mary, Williamsburg, VA 23185, USA

E-mail: eemikh@wm.edu

Received 15 December 2011, in final form 20 January 2012
Published 8 June 2012
Online at stacks.iop.org/JPhysB/45/124015

Abstract
We report on the generation of pulses of a low-frequency squeezed vacuum with noise suppression >2 dB below the standard quantum limit in a hot resonant ^{87}Rb vapour with polarization self-rotation. We demonstrate the possibility of precisely controlling the temporal profile of the squeezed noise quadrature by applying a calibrated longitudinal magnetic field, without degrading the maximum amount of squeezing.

(Some figures may appear in colour only in the online journal)

Growing interest in practical realizations of quantum information (QI) technology stimulates a broad exploration of various optimal protocols and infrastructures. One of the leading approaches is based on using optical fields as QI carriers that can be strongly coupled with resonant matter systems, such as atoms (warm or cold) [1–5], 'atom-like' defects in solid-state systems (such as nitrogen vacancy centres in diamond [6]) and nanostructures (such as quantum dots [7]). While many initial QI protocols relied on qubits formed by individual single photons, continuous variable approaches have become a promising alternative [8, 9]. In this paper, we demonstrate an important tool for continuous variable QI, namely a source of pulsed squeezed vacuum with reliable and simple control over the temporal output mode.

Any experimental implementation of continuous variable measurements or operations requires precise knowledge, or better yet, active control over the spatial and temporal profile of the involved optical fields. It becomes important, for example, for reliably reconstructing the quantum states [10], and for matching the bandwidth of an optical signal with the linewidth of a resonant light–atom interaction to achieve optimal coupling [3]. Good examples of the latter use of temporal pulse shaping can be found in realizations of maximally efficient quantum memory in atomic ensembles [2, 11]. Recent comprehensive theoretical studies by Gorshkov *et al* considered a wide range of potential quantum memory protocols [12–16], such as electromagnetically induced transparency (EIT) in a cavity and in free space, far-off-resonant Raman and a variety of spin-echo methods including ensembles enclosed in a cavity, inhomogeneous broadening and high-bandwidth non-adiabatic storage. Theoretically, high optical depth is necessary to achieve a storage efficiency close to 100% for most of these memories [12]. In practice, however, residual absorption and competing nonlinear processes make atomic ensembles with moderate optical depths most practical. In these situations, shaping of quantum optical signals into predetermined temporal envelopes may be required to achieve optimal efficiency. For example, for EIT-based quantum memories, the efficiency of quantum storage for a given optical depth is fundamentally limited by the balance between the compression of an optical pulse inside the limited length of an atomic ensemble and the width of the transparency spectral window. Thus, the temporal profile of signal and/or control optical fields must be tailored to minimize losses and store the signal with optimal efficiency [17–19].

Traditionally, squeezed light is produced via parametric down-conversion in nonlinear crystals [20]. The development of proper periodic poling masks for $KTiOPO_4$ crystals (PPKTP) enabled efficient quasi-phase-matched down-conversion around 800 nm, and made possible the development of a new generation of solid-state sources for single photons and continuous squeezed and entangled fields at the frequency of the Rb D_1 line. However, a typical spectral bandwidth of the nonlinear optical conversion in such a crystal is rather broad (around a few nm). At the same time, the bandwidths of many light–atom coherent interactions, such as EIT or Raman resonances, do not often exceed a few MHz. For efficient

[1] Author to whom any correspondence should be addressed.

interfacing with these systems, the squeezing sources need a significant reduction of technical noise at these low sideband frequencies. While it is possible to achieve squeezing at sub-MHz frequencies in nonlinear crystals using a combination of narrow-band powerful pump lasers, high-quality cavities and sophisticated electronics for active stabilization and feedback [21–23], this remains a very challenging technical task and requires a significant amount of resources and lab space. Nevertheless, PPKTP-based sources of squeezed vacuum have been successfully integrated with quantum memories in Rb atoms: both under EIT conditions in both cold and hot Rb atoms [24–27], and for the far-off-resonance Raman interactions [28]. Generation of pulsed squeezed vacuum fields using parametric down-conversion-based squeezing methods is also non-trivial. Since these cavity-based crystal squeezers operate in the CW regime and generate a continuous squeezed vacuum field, the pulses have been formed externally, using either mechanical choppers or acousto-optical modulators (AOM). Either of these approaches has serious drawbacks: an additional optical element such as an AOM introduces additional losses and may distort the spatial mode of the generated field due to thermal nonhomogeneities in its nonlinear crystal. Mechanical choppers, such as rotating slits, do not add any losses but produce only rectangular temporal envelopes of fixed duration, which are not ideal for many experiments.

As an alternative to crystal squeezers, optical nonlinearities in resonant atomic media can lead to the generation of non-classical optical fields as well. For example, two-mode squeezed and entangled optical fields were produced as a result of non-degenerate four-wave mixing [29–33] with capabilities of nanosecond-long squeezed pulse generation [34]. A similar interaction for the degenerate case leads to the generation of a resonant broad-band quadrature-squeezed vacuum optical field [35], commonly referred to as polarization self-rotation (PSR) squeezing. This method relies on the strong interaction between two linear polarizations of a near-resonant optical field propagating through an ensemble of resonant atoms. In the case of an elliptically polarized input, the differential light shifts of various Zeeman transitions result in circular birefringence of the atomic vapour and in the rotation of the polarization ellipse by an angle proportional to the input ellipticity [36–39]. An input linear polarization is not rotated, but the same nonlinear interaction is manifested in strong cross-phase modulation between the two orthogonal components (the strong input laser field and the orthogonal vacuum field). Even though the pump laser field propagates through the atoms unaffected, the orthogonally polarized vacuum field becomes quadrature squeezed [40–44]. This method is particularly attractive for applications involving narrow-band coherent light–atom processes, since quantum noise suppression at noise sideband frequencies down to 20 kHz has recently been demonstrated [41]. Other advantages of this method include the relative simplicity of the experimental setup, moderate requirements for pump laser power (a few mW), automatic matching of the wavelength of the generated squeezed field to the corresponding atomic transition wavelength and the possibility of producing pulses

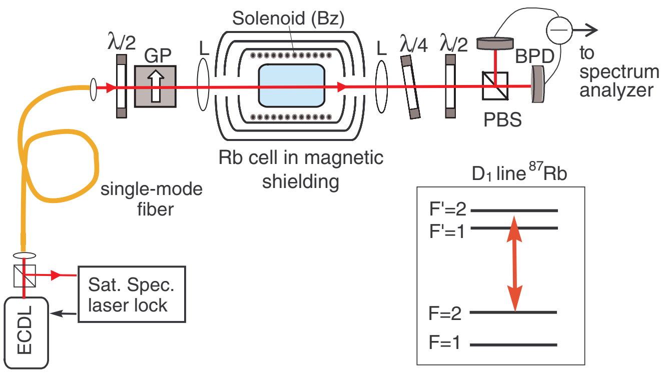

Figure 1. Experimental setup. The description of components is provided in the text.

of squeezed light by modulating the intensity of the pump laser [43].

In this paper, we investigate the modification of quantum fluctuations of a vacuum optical field after propagating through a Rb vapour under PSR conditions in the presence of a magnetic field. In this experiment, we demonstrate that a longitudinal magnetic field allows for good control over the temporal profile of the generated squeezed field, and thus such a setup can be used as a source of pulsed squeezed vacuum with programmable pulse shapes. This method offers important advantages since it does not change the angle of the squeezing quadrature with respect to the local oscillator (LO), and thus allows convenient pulse shape formation without the need to adjust this angle as well. Also, a modest magnetic field does not affect the strong pump field. Thus, this field can be used afterwards as a LO that intrinsically has the same spatial profile as the squeezing beam.

1. Experimental arrangement

The experimental setup is depicted in figure 1. The output of an external cavity diode laser (ECDL) is tuned to the ^{87}Rb D_1 line $F_g = 2 \rightarrow F_e = 2$ transition and actively locked to this transition using a saturation spectroscopy dither lock. The laser output is sent through a polarization-maintaining single-mode fibre to clean its spatial mode, achieving an axially symmetric Gaussian intensity distribution. Then light passes through a half-waveplate and Glan-laser polarizer (GP) combination, which serves as a power attenuator and, most importantly, produces a high-quality linearly polarized pump laser beam. The laser beam is focused with a lens (L) ($f = 400$ mm) to achieve a 100 μm beam waste approximately in the centre of the 75 mm-long Pirex cell with isotopically pure ^{87}Rb. The cell is maintained at 66 °C, corresponding to an atomic number density of 5.4×10^{11} cm^{-3}, which we found experimentally to give the best noise suppression in squeezed vacuum. The cell is surrounded by a three-layer μ-metal magnetic shield and placed inside a solenoid which gives us precise control over the internal longitudinal magnetic field. After the cell, we collimate the laser beam with a second lens ($f = 300$ mm). For squeezing detection, the beam polarization is rotated by 45° with respect to the

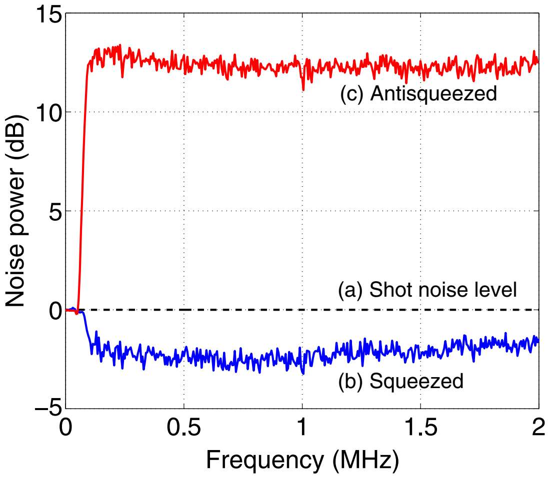

Figure 2. Typical noise spectrum of squeezed and anti-squeezed quadratures. Laser pump power = 7.0 mW. RBW = 10 kHz.

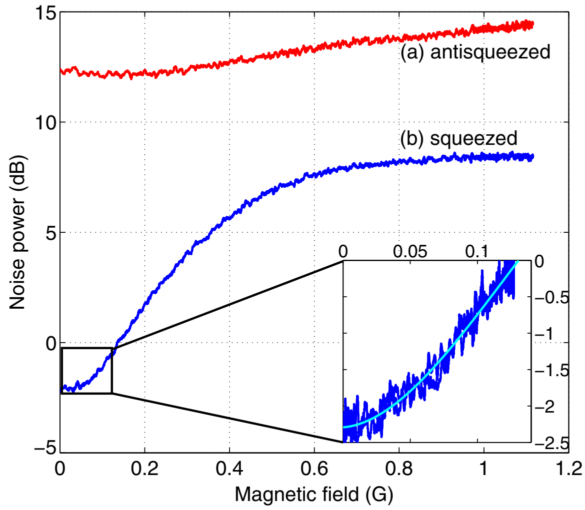

Figure 3. Noise power (dB) of (a) anti-squeezed and (b) squeezed quadratures versus the applied longitudinal magnetic field. Inset zooms in on small fields used for this experiment. The SA is set to 1 MHz central frequency with the RBW = 100 kHz.

axis of a polarizing beam splitter (PBS) using another half-waveplate, to achieve a 50/50 splitting ratio. After the PBS, the two split laser beams are directed to a balanced photo detector (BPD). Such a combination of PBS and BPD makes a very stable homodyne detector, because the phase between the linearly polarized pump beam (used as LO) and the orthogonally polarized squeezed vacuum is fixed and both fields share the same path. This setup was described in [44] and provides superior homodyne phase stability compared to our previous detection scheme [41, 42] which separated the LO and squeezing beam paths. Additionally, the overlap of the squeezing beam and LO is 100% since they are essentially the same beam and travel together until the last PBS. This increases detection efficiency and has allowed squeezing levels of up to 3 dB in similar setups [44]. The output of the BPD goes to a spectrum analyser (SA). The fine control over the measured noise quadrature angle is obtained with a quarter-waveplate, which is placed after the collimating lens and set in such a way that the ordinary and extraordinary axes coincide with the laser beam polarizations. In this arrangement, a small tilt of the quarter-waveplate introduces a controllable phase shift between the squeezed vacuum and LO beam.

In the absence of the magnetic field, we observe a suppression of the quantum noise in the vacuum field below the standard quantum limit (shot noise). This suppression exceeds 2 dB and spans from around 100 kHz to several MHz (see figure 2). We calibrate to the shot noise level by inserting a polarizer after the cell, which completely rejects the squeezed vacuum field and transmits only the LO field. Weak absorption in this polarizer decreases the shot noise level by about 0.2 dB; consequently, the actual/corrected amount of squeezing is higher by this number. The total optical loss in the squeezed vacuum path is equal to 10% (3% at the output window of the cell, 7% at the steering mirrors, collimating lens and balancing PBS); we also estimate the quantum efficiency of our photo diodes to be 95%. Taking into account all of these factors, we infer that our squeezer produces around 3.6 dB of squeezing, from which we are able to detect only 2.3 dB due to losses. Although the inferred 3.6 dB value is still lower than the theoretically predicted 6 dB by Matsko *et al* [45], our squeezer is reasonably close to predicted values, and one expects to see even higher squeezing with cold atoms in a magneto-optical trap [46]. We choose to report only the experimentally measured values of squeezing and do not use the above corrections (even the shot noise reduction) anywhere in the paper.

One possible way to modulate the noise level of the PSR squeezing is by controlling the input pump power. In particular, lowering the pump power degrades and eventually kills the squeezing process, and thus makes it possible to shape the noise pulses [43]. However, this variation of the pump laser intensity makes it difficult to reuse the same beam as a LO and accurately measure the quantum noise levels. This problem can be alleviated by using an independent LO field, but at the price of the increased complexity of the experiment, a lower quantum detection efficiency due to the imperfect overlap of the LO and squeezing beams, and a reduced homodyne phase stability. In addition, we note that one cannot modulate the light signal after it is already squeezed due to the resulting degradation of the noise suppression.

Here we demonstrate a novel approach to squeezing manipulation which avoids these drawbacks. We modify the quantum noise quadrature level resulting from the squeezing process by changing the longitudinal magnetic field (B_z) applied with the solenoid. Figure 3 shows measurements of the minimum (squeezed) and maximum (anti-squeezed) noise quadratures as functions of the applied longitudinal magnetic field. It is clear that the squeezed quadrature has a strong dependence on the magnetic field, while the anti-squeezed quadrature noise level has a much weaker response. A similar increase of intensity noise with magnetic field has been previously reported for weak optical fields [47]. By modifying B_z, we can change the squeezing level from a maximally squeezed state to the shot noise limited level (and beyond). Thus, the B_z dependence on time translates to a squeezing noise time dependence. Both the squeezing and anti-squeezing noise

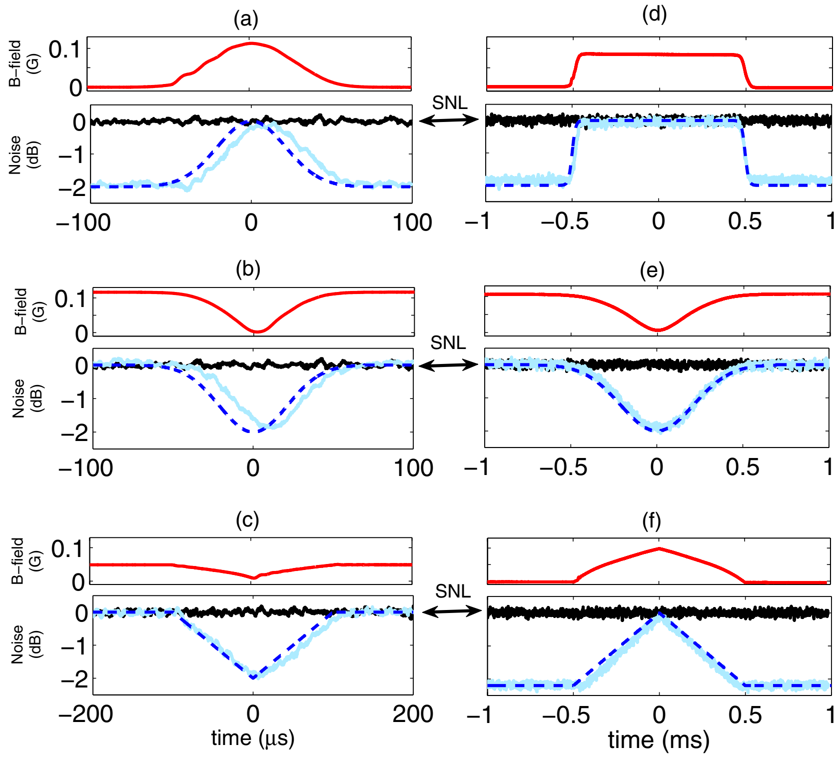

Figure 4. Modulation of the quantum noise with different pulse shapes. Top plots: magnetic field pulses applied to the atoms. Bottom plots: resultant squeezed noise pulses compared with the shot noise limit (SNL). Desired noise pulse shapes shown with dashed lines were Gaussian (a, b and e), triangular (c and f) and square (d).

levels have a nonlinear response to the longitudinal magnetic field (see figure 3) which must be taken into account for the generation of an arbitrary pulse shape.

There are several remarkable features of the observed magnetic field dependence. First, we verified that the change in minimum noise quadrature caused by the applied magnetic field is not accompanied by any changes in its phase with respect to the LO. This means that any squeezing pulses formed by changing the magnetic field will have a uniform phase with no chirping. We also note that the transverse magnetic field has a much weaker effect on the squeezed quantum noise. In particular, we observed no measurable deterioration of quantum noise suppression due to transverse magnetic fields up to several Gauss, even though this is a much stronger field than we apply in the longitudinal direction.

To provide some intuitive explanation of the magnetic field effect on the quadrature noise, one has to consider the effects of Zeeman shifts of the relevant magnetic sublevels. In the simplified model developed in [35], the self-rotation of the elliptical polarization is caused by a circular birefringence induced by a differential light-shift due to unbalanced intensities of two circular polarizations. For a linearly polarized pump field, which can be decomposed into two circular components of equal intensity, all the Zeeman sublevels are shifted equally, and the self-rotation mechanism serves as a 'quantum feedback' for quantum fluctuations. The additional longitudinal magnetic field breaks the degeneracy of the magnetic sublevels, producing non-zero phase shift between two circular components and, as a result, the nonlinear Faraday rotation of the original polarization [48]. It is important to note that the overall rotation of the linear pump polarization due to this effect is rather small and does not modify the shot noise level for small ($B < 0.2$ G) magnetic fields. We also verified that this rotation cannot explain the deterioration of squeezing since it cannot be compensated for by optimizing the angles of the half- and quarter-waveplates at the detection stage. At the same time, the difference in acquired phases for different spectral components of the vacuum field results in a non-stationary minimum quadrature angle and leads to an overall reduction of detectable squeezing. This simple model may also explain the weak effect of the transverse magnetic field. For this so-called Voight configuration, the polarization rotation is caused by linear dichroism of the atomic medium [48]. This effect is quadratic in Zeeman shift and thus is significantly weaker than the rotation in the Faraday configuration.

2. Quadrature-noise pulse shaping

To demonstrate the capabilities of our method, we chose several different temporal profiles with different parameters for the output squeezed vacuum field. Figure 4 shows a few example pulse shapes: (a) a positive Gaussian pulse of 50 μs duration, (b) a 50 μs negative Gaussian pulse, (c) a negative 200 μs triangular pulse, (d) a positive 1 ms square pulse, (e) a negative 1 ms Gaussian pulse and (f) a positive 1 ms triangular pulse. Here, pulses deemed 'positive' start at a maximally squeezed level and show an increase in noise up to shot noise, while for the 'negative' pulses, the measured noise starts at

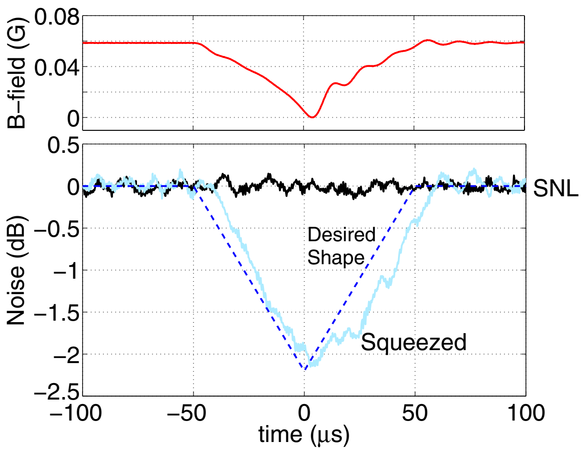

Figure 5. A 100 μs triangular pulse of squeezed noise (the same coding conventions as in figure 4). Limits of the current supply bandwidth cause visible oscillations in the magnetic field which show up in the squeezed spectrum.

the shot noise and then drops to the maximum squeezing level. The desired profile can be reliably reproduced in the measured spectral noise power by calibrating the effect of the magnetic field on the squeezed noise levels. We can use this to determine the transfer function and thus calculate the magnetic field pulses required to produce the desired noise pulse shapes.

We see an excellent mapping from the desired to observed pulse shapes, importantly with no degradation of the maximally squeezed noise quadratures, with the lowest noise levels recorded (maximum squeezing) always occurring at zero magnetic field. The applied magnetic field is chosen so that the quadrature noise moves between the maximally squeezed level (≈ -2.3 dB) and the shot noise level, following the pulse shape we desire. The pulses are smooth and continuous and we have easy control over their duration and repetition rate.

The shortest generated and detected pulses are on the order of 50 μs, which is limited by some electronics available for the experiment. During the measurements of the squeezing pulses above, we set the SA central frequency to 1 MHz, the resolution bandwidth (RBW) to 100 kHz and video bandwidth (VBW) to 3 MHz while we monitored the time-dependent noise level with an oscilloscope. The SA bandwidth setting naturally limits the maximum bandwidth of the pulses or shortest possible detected pulse. However, the main limitation on pulse duration was set by the homemade controllable current source which was used to control the solenoid current. The bandwidth of this current source was limited to about 10 kHz and for shorter pulses, it distorted the programmed pulse shapes by adding unwanted transient effects. We can see the ripples of the set current in figure 5 when the signal bandwidth exceeds the instrumental one. Note however that the detected squeezing accurately follows the distorted magnetic pulse shape, illustrating that it can potentially be modulated much faster. To avoid ring-down oscillations, we smooth the sharp fronts of the input rectangular pulse (see figure 4(d)).

3. Conclusion

In summary, we have studied the effect of an external magnetic field on the PSR vacuum squeezing generated in a hot ^{87}Rb vapour. We found that the longitudinal magnetic field degrades the squeezing, increasing detected noise levels in the squeezed quadrature roughly linearly with applied magnetic field strength (for small fields) but without changing this quadrature angle with respect to the LO. We demonstrated that we can use this dependence to generate pulses of the squeezed vacuum with arbitrary temporal profiles. The advantages of the proposed pulsed squeezing generation method are its simplicity and robustness, good matching of the squeezing parameters to narrow coherent atomic resonances (like EIT or Raman transitions) and the possibility of using the pump field as a LO for perfect spatial mode matching. This technique is thus suitable for time encoding of the quantum states for quantum communication and memory applications.

Acknowledgments

The authors thank Gleb Romanov and Robinjeet Singh for their assistance with the experiment and for useful discussions. This research was supported by NSF grant PHY-0758010.

References

[1] Kimble H J 2008 The quantum internet *Nature* **453** 1023–30

[2] Lvovsky A I, Sanders B C and Tittel W 2009 Optical quantum memory *Nature Photon.* **3** 706–14

[3] Hammerer K, Sørensen A S and Polzik E S 2010 Quantum interface between light and atomic ensembles *Rev. Mod. Phys.* **82** 1041–93

[4] Simon C *et al* 2010 Quantum memories *Eur. Phys. J.* D **58** 1–22

[5] Sangouard N, Simon C, de Riedmatten H and Gisin N 2011 Quantum repeaters based on atomic ensembles and linear optics *Rev. Mod. Phys.* **83** 33–80

[6] Dutt M V G, Childress L, Jiang L, Togan E, Maze J, Jelezko F, Zibrov A S, Hemmer P R and Lukin M D 2007 Quantum register based on individual electronic and nuclear spin qubits in diamond *Science* **316** 1312–6

[7] Cortez S, Krebs O, Laurent S, Senes M, Marie X, Voisin P, Ferreira R, Bastard G, Gérard J-M and Amand T 2002 Optically driven spin memory in *n*-doped InAs–GaAs quantum dots *Phys. Rev. Lett.* **89** 207401

[8] Cerf N J, Leuchs G and Polzik E S (ed) 2007 *Quantum Information with Continuous Variables of Atoms and Light* (London: Imperial College Press)

[9] Andersen U L, Leuchs G and Silberhorn C 2010 Continuous-variable quantum information processing *Laser Photon. Rev.* **4** 337–54

[10] Lvovsky A I and Raymer M G 2009 Continuous-variable optical quantum-state tomography *Rev. Mod. Phys.* **81** 299–332

[11] Novikova I, Walsworth R L and Xiao Y 2011 Electromagnetically induced transparency-based slow and stored light in warm atoms *Laser Photon. Rev.* at press

[12] Gorshkov A V, André A, Fleischhauer M, Sørensen A S and Lukin M D 2007 Universal approach to optimal photon storage in atomic media *Phys. Rev. Lett.* **98** 123601

[13] Gorshkov A V, André A, Lukin M D and Sørensen A S 2007 Photon storage in Λ-type optically dense atomic media: I. Cavity model *Phys. Rev.* A **76** 033804
[14] Gorshkov A V, André A, Lukin M D and Sørensen A S 2007 Photon storage in Λ-type optically dense atomic media: II. Free-space model *Phys. Rev.* A **76** 033805
[15] Gorshkov A V, André A, Lukin M D and Sørensen A S 2007 Photon storage in Λ-type optically dense atomic media: III. Effects of inhomogeneous broadening *Phys. Rev.* A **76** 033806
[16] Gorshkov A V, Calarco T, Lukin M D and Sørensen A S 2008 Photon storage in Λ-type optically dense atomic media: IV. Optimal control using gradient ascent *Phys. Rev.* A **77** 043806
[17] Novikova I, Gorshkov A V, Phillips D F, Sørensen A S, Lukin M D and Walsworth R L 2007 Optimal control of light pulse storage and retrieval *Phys. Rev. Lett.* **98** 243602
[18] Novikova I, Phillips N B and Gorshkov A V 2008 Optimal light storage with full pulse-shape control *Phys. Rev.* A **78** 021802
[19] Zhang S, Zhou S, Loy M M T, Wong G K L and Shengwang D 2011 Optical storage with electromagnetically induced transparency in a dense cold atomic ensemble *Opt. Lett.* **36** 4530–2
[20] Bachor H-A and Ralph T C 2004 *A Guide to Experiments in Quantum Optics* 2nd edn (New York: Wiley-VCH)
[21] Hétet G, Glöckl O, Pilypas K A, Harb C C, Buchler B C, Bachor H-A and Lam P K 2007 Squeezed light for bandwidth-limited atom optics experiments at the rubidium D1 line *J. Phys. B: At. Mol. Opt. Phys.* **40** 221–6
[22] Takeno Y, Yukawa M, Yonezawa H and Furusawa A 2007 Observation of −9 dB quadrature squeezing with improvement of phase stability in homodyne measurement *Opt. Express* **15** 4321–7
[23] Burks S, Ortalo J, Chiummo A, Jia X, Villa F, Bramati A, Laurat J and Giacobino E 2009 Vacuum squeezed light for atomic memories at the D2 cesium line *Opt. Express* **17** 3777–81
[24] Appel J, Figueroa E, Korystov D, Lobino M and Lvovsky A I 2008 Quantum memory for squeezed light *Phys. Rev. Lett.* **100** 093602
[25] Honda K, Akamatsu D, Arikawa M, Yokoi Y, Akiba K, Nagatsuka S, Tanimura T, Furusawa A and Kozuma M 2008 Storage and retrieval of a squeezed vacuum *Phys. Rev. Lett.* **100** 093601
[26] Figueroa E, Lobino M, Korystov D, Appel J and Lvovsky A I 2009 Propagation of squeezed vacuum under electromagnetically induced transparency *New J. Phys.* **11** 013044
[27] Arikawa M, Honda K, Akamatsu D, Nagatsuka S, Akiba K, Furusawa A and Kozuma M 2010 Quantum memory of a squeezed vacuum for arbitrary frequency sidebands *Phys. Rev.* A **81** 021605
[28] Jensen K, Wasilewski W, Krauter H, Fernholz T, Nielsen B M, Owari M, Plenio M B, Serafini A, Wolf M M and Polzik E S 2011 Quantum memory for entangled continuous-variable states *Nature Phys.* **7** 13–6
[29] Slusher R E, Hollberg L W, Yurke B, Mertz J C and Valley J F 1985 Observation of squeezed states generated by four-wave mixing in an optical cavity *Phys. Rev. Lett.* **55** 2409–12
[30] Shahriar M S and Hemmer P R 1998 Generation of squeezed states and twin beams via non-degenerate four-wave mixing in a λ system *Opt. Commun.* **158** 273–86
[31] Boyer V, Marino A M, Pooser R C and Lett P D 2008 Entangled images from four-wave mixing *Science* **321** 544–7
[32] McCormick C F, Marino A M, Boyer V and Lett P D 2008 Strong low-frequency quantum correlations from a four-wave-mixing amplifier *Phys. Rev.* A **78** 043816
[33] Wasilewski W, Fernholz T, Jensen K, Madsen L S, Krauter H, Muschik C and Polzik E S 2009 Generation of two-mode squeezed and entangled light in a single temporal and spatial mode *Opt. Express* **17** 14444–57
[34] Agha I H, Giarmatzi C, Glorieux Q, Coudreau T, Grangier P and Messin G 2011 Time-resolved detection of relative-intensity squeezed nanosecond pulses in an ^{87}Rb vapor *New J. Phys.* **13** 043030
[35] Matsko A B, Novikova I, Welch G R, Budker D, Kimball D F and Rochester S M 2002 Vacuum squeezing in atomic media via self-rotation *Phys. Rev.* A **66** 043815
[36] Davis W V, Gaeta A L and Boyd R W 1992 Polarization-ellipse rotation by induced gyrotropy in atomic vapors *Opt. Lett.* **17** 1304–6
[37] Rochester S M, Hsiung D S, Budker D, Chiao R Y, Kimball D F and Yashchuk V V 2001 Self-rotation of resonant elliptically polarized light in collision-free rubidium vapor *Phys. Rev.* A **63** 043814
[38] Novikova I, Matsko A B and Welch G R 2002 Large polarization self-rotation in rubidium vapour: application for squeezing of electromagnetic vacuum *J. Mod. Opt.* **49** 2565–81
[39] Horrom T, Balik S, Lezama A, Havey M D and Mikhailov E E 2011 Polarization self-rotation in ultracold atomic ^{87}Rb *Phys. Rev.* A **83** 053850
[40] Ries J, Brezger B and Lvovsky A I 2003 Experimental vacuum squeezing in rubidium vapor via self-rotation *Phys. Rev.* A **68** 025801
[41] Mikhailov E E and Novikova I 2008 Low-frequency vacuum squeezing via polarization self-rotation in Rb vapor *Opt. Lett.* **33** 1213–5
[42] Mikhailov E E, Lezama A, Noel T W and Novikova I 2009 Vacuum squeezing via polarization self-rotation and excess noise in hot Rb vapors *J. Mod. Opt.* **56** 1985–92
[43] Agha I H, Messin G and Grangier P 2010 Generation of pulsed and continuous-wave squeezed light with ^{87}Rb vapor *Opt. Express* **18** 4198–205
[44] Barreiro S, Valente P, Failache H and Lezama A 2011 Polarization squeezing of light by single passage through an atomic vapor *Phys. Rev.* A **84** 033851
[45] Matsko A B, Novikova I, Welch G R, Budker D, Kimball D F and Rochester S M 2002 Vacuum squeezing in atomic media via self-rotation *Phys. Rev.* A **66** 043815
[46] Horrom T, Lezama A, Balik S, Havey M D and Mikhailov E E 2011 Quadrature noise in light propagating through a cold ^{87}Rb atomic gas *J. Mod. Opt.* **58** 1936–41
[47] Li H, Sautenkov V A, Varzhapetyan T S, Rostovtsev Y V and Scully M O 2008 Atomic noise spectra in nonlinear magneto-optical rotation in a rubidium vapor *J. Opt. Soc. Am.* B **25** 1702–7
[48] Budker D, Gawlik W, Kimball D F, Rochester S M, Yashchuk V V and Weis A 2002 Resonant nonlinear magneto-optical effects in atoms *Rev. Mod. Phys.* **74** 1153–201